Int. J. Electrochem. Sci., 11 **(2016)** 432 - 445

International Journal of
ELECTROCHEMICAL
SCIENCE
www.electrochemsci.org

First-principles GGA+U Study on Structural and Electronic Properties in $LiMn_{0.5}Ni_{0.5}O_2$, $LiMn_{0.5}Co_{0.5}O_2$ and $LiCo_{0.5}Ni_{0.5}O_2$

B.Liu, B.Xu[*] *, M. S. Wu and C. Y. Ouyang*

Department of Physics, Jiangxi Normal University, Nanchang, 330022, China
[*]E-mail: bxu4@mail.ustc.edu.cn

Received: 9 October 2015 / *Accepted:* 31 October 2015 / *Published:* 1 December 2015

The structural and electronic properties of lithium mixed transition metal oxides $LiMn_{0.5}Ni_{0.5}O_2$, $LiMn_{0.5}Co_{0.5}O_2$ and $LiCo_{0.5}Ni_{0.5}O_2$ are studied by using first-principles calculations based on the density functional theory. Results show that the rhombohedral structure with $R\bar{3}m$ space group is the most stable configuration for $LiMn_{0.5}Ni_{0.5}O_2$, $LiMn_{0.5}Co_{0.5}O_2$ and $LiCo_{0.5}Ni_{0.5}O_2$ compounds, indicating that the mixture of cations in the transition metal layers is help to suppress the Jahn-Teller distortion for the Ni- and Mn-containing oxides. Electronic structure calculations suggest that all the three compounds are semiconducting with small band gaps. In the Mn-containing oxides, $LiMn_{0.5}Ni_{0.5}O_2$, $LiMn_{0.5}Co_{0.5}O_2$, charge transfers from Mn ion to Co or Ni ions, resulting in Mn^{4+} and Ni^{2+} or Co^{2+}. Charge transfer could be used to explain the suppression of the Jahn-Teller effect. As charge transfer cannot be observed between Co and Ni ions, the Jahn-Teller distortion still exists in $LiCo_{0.5}Ni_{0.5}O_2$, but mitigated to some extent. The further electronic configurations, density of states and magnetic moments are also discussed. In addition, formation energy calculations show that $LiMn_{0.5}Ni_{0.5}O_2$, $LiMn_{0.5}Co_{0.5}O_2$ and $LiCo_{0.5}Ni_{0.5}O_2$ compounds are thermodynamic stable when compared to the basic layered $LiMO_2$ (M = Co, Mn, Ni), which means that the mixture of cations in the lithium transition metal oxides could be formed.

Keywords: First-principles, Jahn-Teller effect, Electronic structure, Cathode material.

1. INTRODUCTION

Development and discovery of cathode materials with superior performance are always the concerned issues for Li-ion battery scientists. Layered $LiCoO_2$ is the conventional and most commonly used cathode material. However, many problems associated with the low practical capacity (130-150 mAh/g) [1], the toxicity of cobalt and the limitation of Co resource restrict the large scale application

of $LiCoO_2$ cathode material. $LiNiO_2$, on the contrary, is considerably less expensive and has a higher initial capacity (200 mAh/g) than $LiCoO_2$ [2]. However, $LiNiO_2$ as cathode material is known to be more difficult to synthesize, which suffers from low reversible capacity and poor cyclability. This is mainly due to the poor structural stability of $LiNiO_2$ compound caused by the Jahn-Teller (JT) effect of active Ni^{3+} ions in the lattice [3]. Manganese oxides are lower cost and less toxic than cobalt or nickel oxides, and have been proved to be safer on overcharge [4]. Thus, lithium manganese oxide cathodes have received much attention. Unfortunately, due to the more complex structure than those of $LiCoO_2$ or $LiNiO_2$, capacity fading, phase instability and structural transformation that occurs with cycling [5-9], there is a distance away from the practical application for the lithium manganese oxide.

Considering the advantages and disadvantages of the basic $LiCoO_2$ or $LiNiO_2$ or $LiMnO_2$, considerable attention has therefore been paid to modify the commercial cathode material $LiCoO_2$, i.e. partial substitution of Co by other transition metal ions such as Ni or Mn. Because Ni and Mn are more abundant and less expensive and less toxic than Co, while they can improve the materials capacity and stability. $LiNiO_2$ is usually mixed with $LiCoO_2$ in unit cell level by applying solid-state chemistry and electrochemistry methods, forming solid solution phase of $LiCo_{1-x}Ni_xO_2$ [10,11]. It was shown experimentally that Co replacement of Ni ions in a reasonable concentration in $LiCo_{1-x}Ni_xO_2$ can suppress the JT distortion of Ni^{3+}, and thus enhance the thermal stability and cycling performance [12]. Stoyanova *et al*. reported that Co can be replaced by Mn to prepare a layered $LiCo_{1-y}Mn_yO_2$ solid solution ($0 < y \leq 0.2$) with a hexagonal lattice [13,14], although Ohzuku *et al*. believed that $LiCoO_2$ was immiscible with $LiMnO_2$ in the whole range of y [15]. Theoretically, Shukla *et al*. reported that the structural transformation from rhombohedral to monoclinic would occur for the Ni- and Co-doped $LiMnO_2$ based on first-principles calculations [16]. On the other hand, in order to improve the stability and capacity of $LiNiO_2$, Mn and Co could also be used to replace the Ni ions. Wang *et al*. have theoretically studied that the JT distortion in $LiNiO_2$ is substantially suppressed by Co atoms that replace Ni atoms in the lattice [17]. More recently, Hao *et al*. have found that Ti doping could further enhance the structural stability of $LiCo_{0.5}Ni_{0.5}O_2$, thus improving the electrochemical properties [18]. Furthermore, Mn ions are easily incorporated into the Ni cation layers to prepare $LiNi_{1-y}Mn_yO_2$. Early work of Rossen *et al*. [19] investigated the solid-state synthesis and electrochemistry of the solid solution $LiMnO_2$-$LiNiO_2$. Ohzuku and Makimura [20] presented recent work on the $LiNi_{0.5}Mn_{0.5}O_2$ system, showing a rhombohedral structure, a sloping discharge profile, and a reversible capacity (150 mAh/g) in the voltage range 2.5-4.3 V. Recently, FTIR and Raman experimental analysis has also confirmed the layered rhombohedral structure for the $LiNi_{0.5}Mn_{0.5}O_2$ [21].

As introduced above, layered $LiMO_2$ (M = Co, Mn, Ni) with mixed metal cations in the transition metal layers shows superior electrochemical and safety behavior to the corresponding basic layered oxide. It is apparent in the research area of lithium battery materials that the underlying structural and electronic properties of lithium transition metal oxides are very complex, but are crucial to the complete understanding of the physical nature of cathode materials. Therefore, the present study utilizes computational techniques based on density functional theory (DFT) to systematically investigate the key issues of structures, electronic structures, charge transfer, electronic configuration, valence states and magnetic moment of $LiMn_{0.5}Ni_{0.5}O_2$, $LiMn_{0.5}Co_{0.5}O_2$ and $LiCo_{0.5}Ni_{0.5}O_2$ system at atomic and electronic level.

2. COMPUTATIONAL METHODOLOGIES

All calculations are performed using the Vienna *ab* initio simulation package (VASP) [22]. The core ion and valence electron interaction are described by the projector augmented wave (PAW) [23] method and the exchange-correlation part is described with the spin-polarized generalized gradient approximation (GGA) with Perdew-Burke-Ernzerhof (PBE) exchange correlation functional [24]. In order to correctly reproduce the electronic structure of the transition metal atoms with 3*d* electrons, GGA+U method is employed [25]. According to the previous studies of Li-ion battery materials [26,27], the effective onsite Coulomb term U_{eff} are set to be 3.5, 3.9 and 5.3 eV for Mn, Co and Ni, respectively.

The convergence tests of the total energy with respect to the *k*-point sampling and energy cutoff have been carefully examined, which ensure that the total energy is converged. The Brillouin zone (BZ) is sampled by using a 3×3×1 Monkhorst–Pack [28] grids for relaxation calculations and a 5×5×2 one for static calculations. Energy cutoff for the plane waves is chosen to be 550 eV. Both the lattice parameters and the ionic positions are fully relaxed. The final forces on all relaxed atoms are less than 0.01 eV/Å. The calculation of the density of states (DOS) is smeared by the Gaussian smearing method with a smearing width of 0.05 eV.

Li*M*O_2 (*M* = Co, Mn, Ni) adopt the α-$NaFeO_2$ structure. The stable form of $LiCoO_2$ is layered rhombohedral structure with symmetry $R\bar{3}m$. However, the monoclinic structures with *C*2/*m* space group symmetry are the stable phases for $LiMnO_2$ and $LiNiO_2$ due to the JT distortion of Mn^{3+} and Ni^{3+}. Since $R\bar{3}m$ and *C*2/*m* space group could be both observed for the Li*M*O_2 compound, we also consider the two phases in the various lithium mixed transition metal oxides. In order to construct the mixed system with 1:1 ratio of atom number for the two transition metal atoms, a 2×2×1 supercell for $R\bar{3}m$ phase, which contains 48 atoms, and a 2×2×2 supercell for *C*2/*m* phase, which contains 32 atoms, are employed in our study. Then, half of the transition metal atoms in each M-O layer are replaced by the other transition metal atoms, because Kim found that the structures of $LiNiO_2$ doping with Co or Mn in the same layer are more stable [29]. For 2×2×1 supercell of $R\bar{3}m$ phase $LiCoO_2$, for example, two Co atoms in each Co-O layer (Co_4O_8) are substituted by Mn atoms, forming the $Co_2Mn_2O_8$ layer. In the end, the $Li_{12}Co_6Mn_6O_{24}$ supercell are obtained for the $LiCo_{0.5}Mn_{0.5}O_2$ $R\bar{3}m$ phase. Similar methods are used to get the $LiCo_{0.5}Ni_{0.5}O_2$, $LiMn_{0.5}Ni_{0.5}O_2$ structures.

In our calculations, we consider both ferromagnetic (FM) and anti-ferromagnetic (AFM) spin configurations as the magnetic atoms play an important role in the electronic properties. It is found that the total energy of the system with AFM ordering is slightly lower than that with FM ordering. Therefore, unless otherwise specified, the results presented in the following sections of this work are according to the AFM configuration. However, our results show that FM or AFM ordering has little influence on the magnetic and valence state of transition metal atoms.

3. RESULTS AND DISCUSSION

3.1 Structures

First, we examine the structures of the lithium mixed transition metal oxides. The structures with different arrangement of the transition metal atoms in both $R\bar{3}m$ and $C2/m$ phases are optimized in our calculations. The most stable structures for $LiMn_{0.5}Ni_{0.5}O_2$, $LiCo_{0.5}Ni_{0.5}O_2$ and $LiMn_{0.5}Co_{0.5}O_2$ are obtained and shown in Fig. 1(a), (b) and (c), respectively. The calculated and experimental lattice parameters are listed in Table 1, where the results available from other works are also given for comparison. It is found that our calculated results are reasonably in agreement with other reports and experimental values.

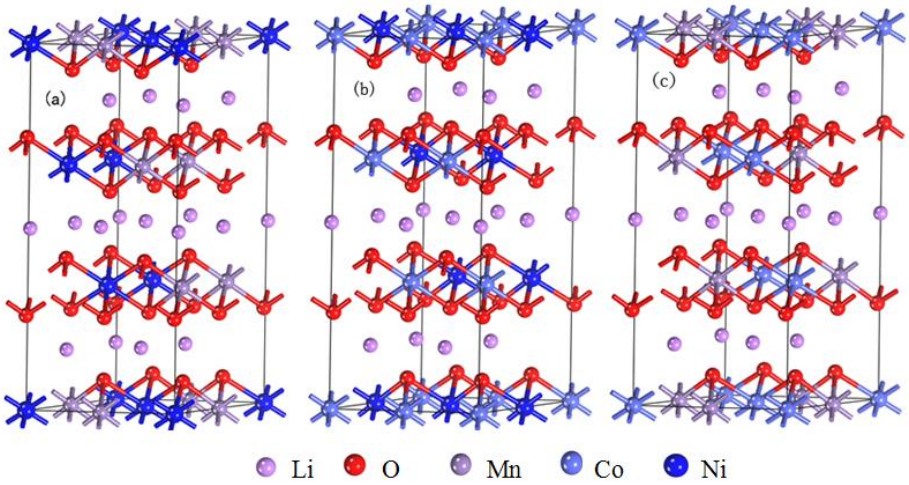

Figure 1. Schematic views of the atomic structures of (a) $LiMn_{0.5}Ni_{0.5}O_2$, (b) $LiCo_{0.5}Ni_{0.5}O_2$ and (c) $LiMn_{0.5}Co_{0.5}O_2$.

Table 1. Lattice parameters(a, b and c in Å), unit cell volume($V/Å^3$) of $LiMn_{0.5}Ni_{0.5}O_2$, $LiCo_{0.5}Ni_{0.5}O_2$, $LiMn_{0.5}Co_{0.5}O_2$.

Compound		a/Å	b/Å	c/Å	c/a	$V/Å^3$
$LiMn_{0.5}Ni_{0.5}O_2$						
This work	GGA+U	2.926	2.926	14.387	4.917	106.69
Calculated [30]	GGA+U	2.940	2.940	14.440	4.912	108.09
Calculated [31]	GGA	2.914	2.914	14.398	4.941	105.88
Experimental [32]		2.881	2.881	14.278	4.956	102.61
$LiCo_{0.5}Ni_{0.5}O_2$						
This work	GGA+U	2.857	2.857	14.207	4.973	100.42
Calculated [18]	GGA+U	2.898	2.898	14.282	4.928	103.87
Experimental [33]		2.845	2.845	14.123	4.964	98.99
$LiMn_{0.5}Co_{0.5}O_2$						
This work	GGA+U	2.986	2.986	14.352	4.806	110.82

As mentioned above, $LiCoO_2$ has the layered $R\bar{3}m$ rhombohedral structure, whereas $LiMnO_2$ and $LiNiO_2$ are monoclinic with $C2/m$ space group due to the JT distortion of Mn and Ni ions. This

means that the JT effect lowers the structural symmetry in the Li*M*O_2 compound. According to our total energy calculations, it is clearly found that $LiMn_{0.5}Ni_{0.5}O_2$, $LiCo_{0.5}Ni_{0.5}O_2$, and $LiMn_{0.5}Co_{0.5}O_2$ all keep the α-$NaFeO_2$ structures, which are rhombohedral with $R\bar{3}m$ symmetry. Obviously, the structural symmetry do not be lowered even if the $LiMn_{0.5}Ni_{0.5}O_2$, $LiCo_{0.5}Ni_{0.5}O_2$, and $LiMn_{0.5}Co_{0.5}O_2$ compounds possess the Mn and Ni ions which are extremely easy to bring the JT effect. Our results are consistent with that of Prasad *et al.*[34], where they indicated that the dopants, such as Co and Fe, could destabilize the monoclinic structure relative to the rhombohedral structure for the $LiMnO_2$ compound. For the lithium mixed transition metal oxides, therefore, the structural distortion resulting from the JT distortion of transition metal atoms are suppressed to some extent. From the application point of view, therefore, the cycling stability of the lithium mixed transition metal oxides should be better than that of $LiNiO_2$ or $LiMnO_2$ due to the higher structural symmetry.

Table 2. Interatomic bonds between transition metal atoms and oxygen atoms in $LiMn_{0.5}Ni_{0.5}O_2$, $LiCo_{0.5}Ni_{0.5}O_2$, $LiMn_{0.5}Co_{0.5}O_2$, and Li*M*O_2 (*M* = Mn, Ni, Co).

Compound	Interatomic bond (Å)		
	Co-O	Ni-O	Mn-O
$LiMn_{0.5}Ni_{0.5}O_2$		2.063	1.948
$LiCo_{0.5}Ni_{0.5}O_2$	1.940	2×2.052/2×1.965/2×1.892	
$LiMn_{0.5}Co_{0.5}O_2$	2.096		1.956
$LiCoO_2$	1.938		
m-$LiNiO_2$		2×2.144/4×1.899	
m-$LiMnO_2$			2×2.356/4×1.952

To further confirm the suppressed effect of mixture of transition metal atoms on the structures, we analyze the interatomic bonds between transition metal atoms and oxygen atoms, as listed in Table 2. In order to facilitate comparison, the results of Li*M*O_2 (*M* = Mn, Ni, Co) are also provided. For $LiCoO_2$ structure, six Co-O bonds in CoO_6 octahedron are all equal to 1.938 Å, which indicates that no JT distortion occurs. Nevertheless, the bond lengths of $LiNiO_2$ and $LiMnO_2$ are divided into two groups, with two long (2.144 Å for $LiNiO_2$ and 2.356 Å for $LiMnO_2$) and four short (1.899 Å for $LiNiO_2$ and 1.952 Å for $LiMnO_2$) bonds, an indication of typical JT type elongation of the octahedron. The calculated values agree well with those from previous report [35], where two long (2.15 Å) and four short (1.90 Å) bonds could be obtained in monoclinic $LiNiO_2$. If two kinds of transition metal atoms are mixed, the situations are significantly different. For the $LiMn_{0.5}Ni_{0.5}O_2$, which includes both Mn and Ni atoms with 1:1 ratio of atom number, the six Ni-O bond lengths in NiO_6 octahedron become very close to each other. The average Ni-O bond length is 2.063 Å, which is between two types of bond lengths in monoclinic $LiNiO_2$. Meanwhile, the Mn-O bond lengths in MnO_6 octahedron of $LiMn_{0.5}Ni_{0.5}O_2$ also tend to the same with the average value of 1.948 Å, very close to the short Mn-O bond lengths in monoclinic $LiMnO_2$. As a result, from the structure point of view, the distortion of MnO_6 and NiO_6 octahedron in $LiMn_{0.5}Ni_{0.5}O_2$ is substantially reduced compared with $LiNiO_2$ and $LiMnO_2$ compounds, and thus the JT effect is evidently suppressed. According to Table 2, similar results could be found for the case of $LiMn_{0.5}Co_{0.5}O_2$. In $LiMn_{0.5}Co_{0.5}O_2$, the six Co-O bond lengths of

CoO_6 octahedron are still equal to each other, whereas the values of 2.096 Å is evidently larger than that in $LiCoO_2$ (1.938 Å), which imply Co ion reduction. The calculated Co-O bond lengths for $LiMn_{0.5}Co_{0.5}O_2$ are very close to that of the case for $LiMn_{0.75}Co_{0.25}O_2$ [36], where the obtained Co-O bond lengths are 2.05 Å. In addition, the equivalent Mn-O bond lengths can also be obtained with 1.956 Å, which is basically equal to the short Mn-O bond lengths in monoclinic $LiMnO_2$.

Different from the case of $LiMn_{0.5}Ni_{0.5}O_2$ and $LiMn_{0.5}Co_{0.5}O_2$, the JT distortion can be found in $LiCo_{0.5}Ni_{0.5}O_2$. Although the six Co-O bond lengths are equal to 1.940 Å, which is almost the same as that in rhombohedral $LiCoO_2$ (1.938 Å), three types of bond lengths are formed for the six Ni-O bonds in the NiO_6 octahedron with 2.052, 1.965 and 1.892 Å for every two, respectively. Large differences among Ni-O bond lengths indicate the local structural distortion of the NiO_6 octahedron, and thus relating with JT effect. On the other hand, it is found that the differences of Ni-O bond lengths are somewhat smaller than that in monoclinic $LiNiO_2$, as listed in Table 2. As a result, the JT effect is mitigated when the Co atoms are incorporated into the $LiNiO_2$ structure.

3.2 Electronic structures

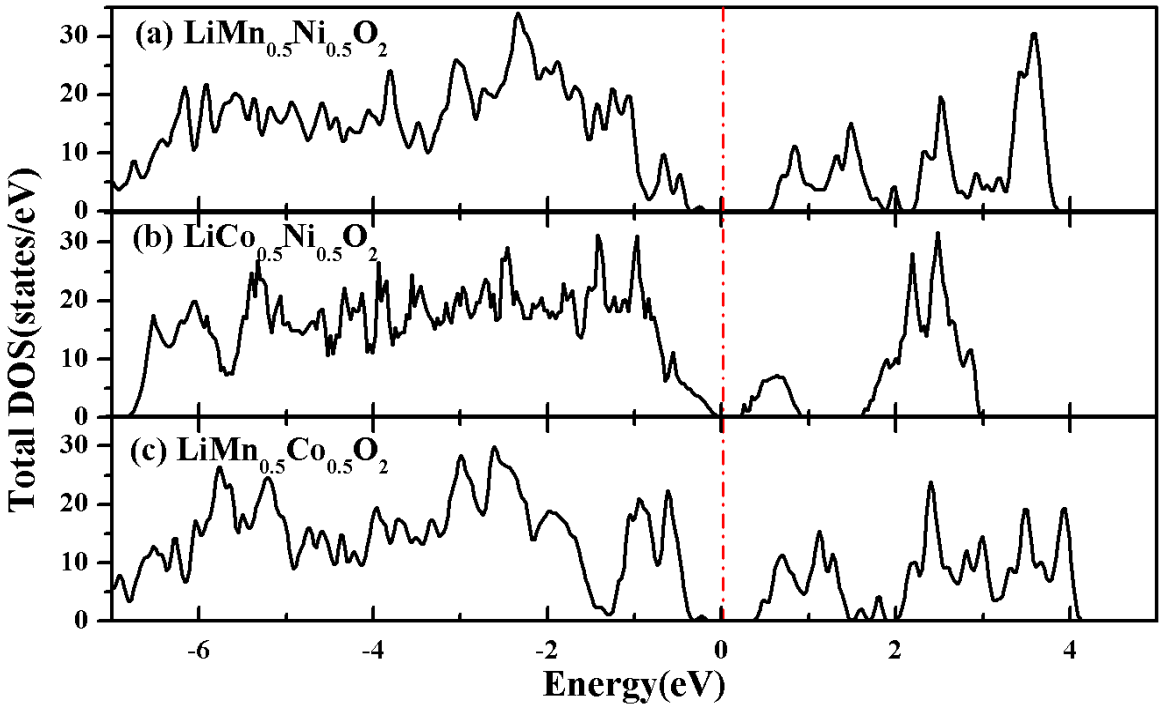

Figure 2. Total density of states of (a) $LiMn_{0.5}Ni_{0.5}O_2$, (b) $LiCo_{0.5}Ni_{0.5}O_2$, and (c) $LiMn_{0.5}Co_{0.5}O_2$ obtained from GGA+U method.

As the electrode materials, the electronic conductivity is important to their performance. The band gap is the key criterion. Figure 2(a)-(c) show the total density of states (TDOS) of $LiMn_{0.5}Ni_{0.5}O_2$, $LiCo_{0.5}Ni_{0.5}O_2$, $LiMn_{0.5}Co_{0.5}O_2$, respectively. From Fig. 2, it is found that the three lithium mixed transition metal oxides all exhibit the semiconducting nature. The energy band gaps are

0.53, 0.23 and 0.33 eV for $LiMn_{0.5}Ni_{0.5}O_2$, $LiCo_{0.5}Ni_{0.5}O_2$ and $LiMn_{0.5}Co_{0.5}O_2$, respectively. The corresponding values are listed in Table 3. The calculated energy band gaps of basic Li*M*O_2 are also provided, which are 1.97, 0.31 and 0.79 eV for $LiCoO_2$, $LiNiO_2$ and $LiMnO_2$, respectively. Therefore, the band gaps of the mixed transition metal compounds are comparable to that of $LiNiO_2$, but smaller than that of $LiMnO_2$ and $LiCoO_2$. Although the DFT methods generally underestimate the band gap of the semiconducting materials to some extent, the small band gaps indicate that electronic conductivity of the three mixed transition metal compounds are not bad, especially better than $LiCoO_2$.

Table 3. Physical properties for the layered structures calculated with the GGA+U method. MM represents the magnetic momentum (in unit μ_B) of transition metal atom, and Eg is energy band gap (in unit eV).

Compound	TM	Valence state	d-Electrons	MM (μ_B)	Eg (eV)
$LiMn_{0.5}Ni_{0.5}O_2$	Mn	+4	t_{2g}^3	3.1	0.53
	Ni	+2	$t_{2g}^6e_g^2$	1.7	
$LiCo_{0.5}Ni_{0.5}O_2$	Co	+3	t_{2g}^6	0	0.23
	Ni	+3	$t_{2g}^6e_g^1$	1.0	
$LiMn_{0.5}Co_{0.5}O_2$	Mn	+4	t_{2g}^3	3.2	0.33
	Co	+2	$t_{2g}^5e_g^2$	2.7	
$LiCoO_2$	Co	+3	t_{2g}^6	0	1.97
m-$LiNiO_2$	Ni	+3	$t_{2g}^6e_g^1$	1.0	0.31
m-$LiMnO_2$	Mn	+3	$t_{2g}^3e_g^1$	3.83	0.79

The detailed electron configurations of the transition metal atoms play an important role in the structural and magnetic properties. The projected density of states (PDOS) of the transition metal atoms could be conveniently used to study the electron configurations. The calculated PDOS of the transition metal atoms for different compounds are described as following. And the physical properties for the lithium transition metal oxides are listed in Table 3. In order to better compare, the results for Li*M*O_2 (*M* = Mn, Ni, Co) are also given.

A. $LiMn_{0.5}Ni_{0.5}O_2$

Figure 3 compares the Mn-3*d* PDOS in $LiMnO_2$ and $LiMn_{0.5}Ni_{0.5}O_2$ compounds. In $LiMnO_2$, the e_g orbital of Mn ion in the spin-up channel splits into two orbitals, namely dx^2-y^2 and dz^2 orbitals. The t_{2g} and dz^2 orbitals in the spin-up channel are occupied, whereas the dx^2-y^2 orbitals in this channel is empty. In addition, the t_{2g} and e_g orbitals in the spin-down channel are entirely empty.

Therefore, the electron configuration of Mn ion is $(t_{2g})^3(e_g)^1$, which clearly indicates that the valence state of Mn ion is +3, namely Mn^{3+}. Furthermore, the Mn^{3+} ions in $LiMnO_2$ are in high spin states, and thus the calculated magnetic moment (MM) is 3.83 μ_B, which is close to 4.0 μ_B. On the other hand, however, Mn ions in $LiMn_{0.5}Ni_{0.5}O_2$ have a $(t_{2g})^3(e_g)^0$ electron configuration, where the Mn-3*d* t_{2g} orbital in the spin-up channel are fully occupied and the other orbitals with both spin states are completely empty, indicating that the Mn ion transfers one electron to its neighboring atoms/ions

and thus forms Mn^{4+}. Correspondingly, the magnetic moment of Mn ion in $LiMn_{0.5}Ni_{0.5}O_2$ is 3.1 μ_B (as seen in Table 3). As the Mn^{4+} has no JT distortion, the Mn-O bond lengths are equal to each other in MnO_6 octahedron of $LiMn_{0.5}Ni_{0.5}O_2$, which could be used to explain the structural difference of MnO_6 octahedron in $LiMnO_2$ and $LiMn_{0.5}Ni_{0.5}O_2$.

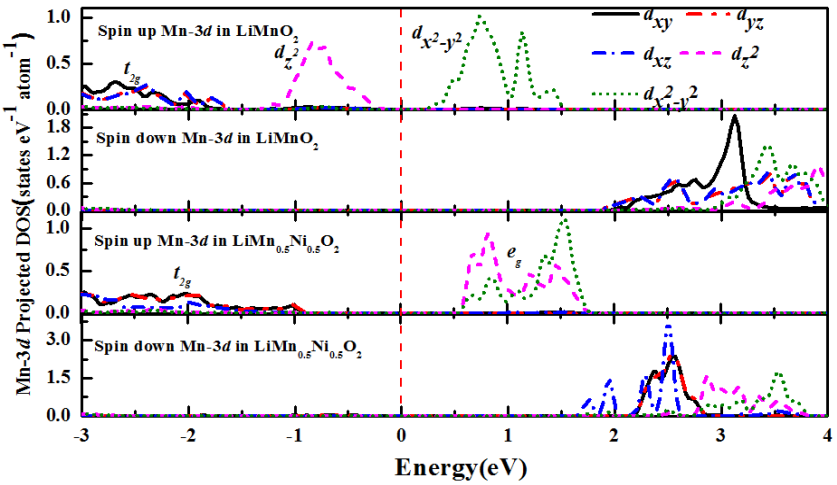

Figure 3. Mn-3*d* PDOS in $LiMnO_2$ and $LiMn_{0.5}Ni_{0.5}O_2$. The triplet and the duplet of the *d*-orbital are denoted as t_{2g} and e_g, respectively. The Fermi levels are all set to be 0 eV.

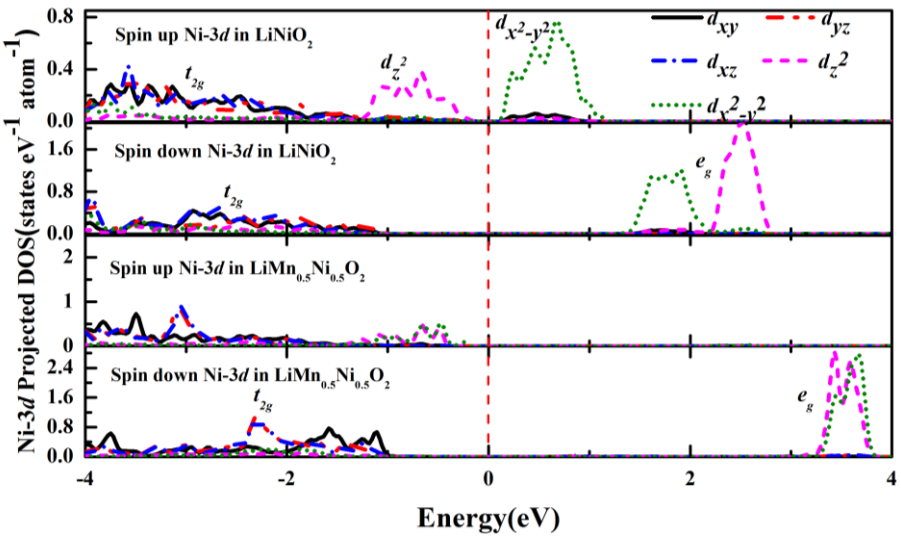

Figure 4. Ni-3*d* PDOS in $LiNiO_2$ and $LiMn_{0.5}Ni_{0.5}O_2$. The triplet and the duplet of the *d*-orbital are denoted as t_{2g} and e_g, respectively. The Fermi levels are all set to be 0 eV.

Figure 4 compares the Ni-3*d* PDOS in $LiNiO_2$ and $LiMn_{0.5}Ni_{0.5}O_2$ compounds. In $LiNiO_2$, the orbitals in the spin-up channel are similar to that of $LiMnO_2$, while the filled t_{2g} orbitals and empty e_g orbitals in the spin-down channel are formed, which is different from that of $LiMnO_2$. Obviously, the electron configuration of Ni ion in $LiNiO_2$ is $(t_{2g})^6(e_g)^1$, and thus forming Ni^{3+}. The magnetic moment

of Ni^{3+} is 1.0 μ_B. When Ni ions are incorporated into $LiMnO_2$ to form $LiMn_{0.5}Ni_{0.5}O_2$, a $(t_{2g})^6(e_g)^2$ electronic configuration could be found. Comparison with the electron configuration of Ni ion in $LiNiO_2$, Ni ion in $LiMn_{0.5}Ni_{0.5}O_2$ gains one electron, which is localized at the dx^2-y^2 orbital of the spin-up channel, thus forming Ni^{2+}. The magnetic moment of Ni^{2+} is calculated to be 1.7 μ_B. With such an electronic configuration, the NiO_6 octahedron are no longer JT active, and the six Ni-O bonds have almost the same bond lengths. These results coincide with the previous LSDA calculations that are performed by Koyama *et al.* [15]

B.$LiMn_{0.5}Co_{0.5}O_2$

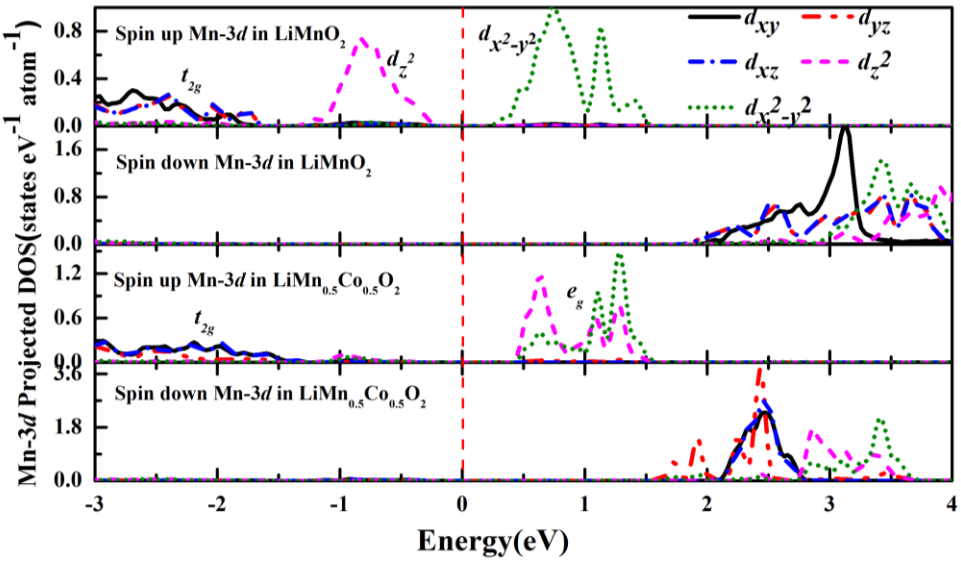

Figure 5. Mn-3*d* PDOS in $LiMnO_2$ and $LiMn_{0.5}Co_{0.5}O_2$. The triplet and the duplet of the *d*-orbital are denoted as t_{2g} and e_g, respectively. The Fermi levels are all set to be 0 eV.

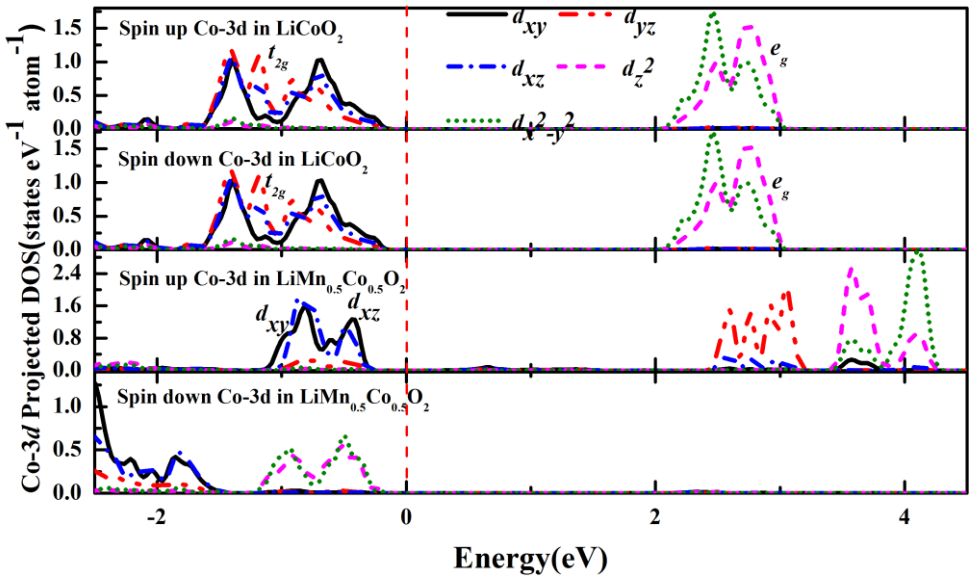

Figure 6. Co-3*d* PDOS in $LiCoO_2$ and $LiMn_{0.5}Co_{0.5}O_2$. The triplet and the duplet of the *d*-orbital are denoted as t_{2g} and e_g, respectively. The Fermi levels are all set to be 0 eV.

Figure 5 shows the Mn-3*d* PDOS in $LiMnO_2$ and $LiMn_{0.5}Co_{0.5}O_2$ compounds. It is found that the results of Mn-3*d* PDOS in $LiMn_{0.5}Co_{0.5}O_2$ is extremely similar to that in $LiMn_{0.5}Ni_{0.5}O_2$. Therefore, the electron configuration of Mn ion in $LiMn_{0.5}Co_{0.5}O_2$ is $(t_{2g})^3(e_g)^0$, and thus coming into being +4 valence state (Mn^{4+}) and 3.2 μ_B magnetic moment (as seen in Table 3). This result is also related with the equal Mn-O bond lengths in $LiMn_{0.5}Co_{0.5}O_2$ due to the JT inactivity of Mn^{4+}.

Due to the full occupation of t_{2g} orbitals and non-occupation of e_g orbitals for Co-3*d* orbitals in $LiCoO_2$ compound, regardless of spin channels (as seen in Fig. 6), which results in the $(t_{2g})^6(e_g)^0$ electron configuration, the valence state and the magnetic moment are +3 and 0 μ_B, respectively, which are in agreement with the results obtained by Xiong *et al.* [37] After the mixing of the Mn and Co atoms in the lithium transition metal oxides with 1:1 atomic ratio, the Co-3*d* PDOS change a lot. All t_{2g} and e_g orbitals with spin down are filled, and two t_{2g} orbitals (*d*xy and *dx*z) with spin up are also occupied. However, the remanent orbials in the spin-up channel are unoccupied. As a result, the $(t_{2g})^5(e_g)^2$ electron configuration is obtained, which results in the +2 valence state and 2.7 μ_B. Combining with the Mn-3*d* characteristic in $LiMn_{0.5}Co_{0.5}O_2$, it can be found that charge transfers from Mn to Co. Our results are basically in agreement with that reported by Prasad *et al.* where the $LiMn_{0.75}Co_{0.25}O_2$ is mainly discussed [36].

C. $LiCo_{0.5}Ni_{0.5}O_2$

Figure 7 and Fig. 8 show the Co-3*d* and Ni-3*d* PDOS. For Co-3*d* PDOS, the occupation of orbitals in $LiCo_{0.5}Ni_{0.5}O_2$ is the same as that in $LiCoO_2$. The same thing happens for Ni-3*d* PDOS. This means that the electron configurations and magnetic moments of Co ion and Ni ion in the $LiCo_{0.5}Ni_{0.5}O_2$ compound do not change when compared with $LiCoO_2$ and $LiNiO_2$. Therefore, the $(t_{2g})^6(e_g)^0$ and $(t_{2g})^6(e_g)^1$ electron configurations for Co^{3+} and Ni^{3+} respectively in $LiCo_{0.5}Ni_{0.5}O_2$ can be obtained (as seen in Table 3), which is in accordance with the experimental observations [33]. In this case, no charge transfer between Co and Ni occurs.

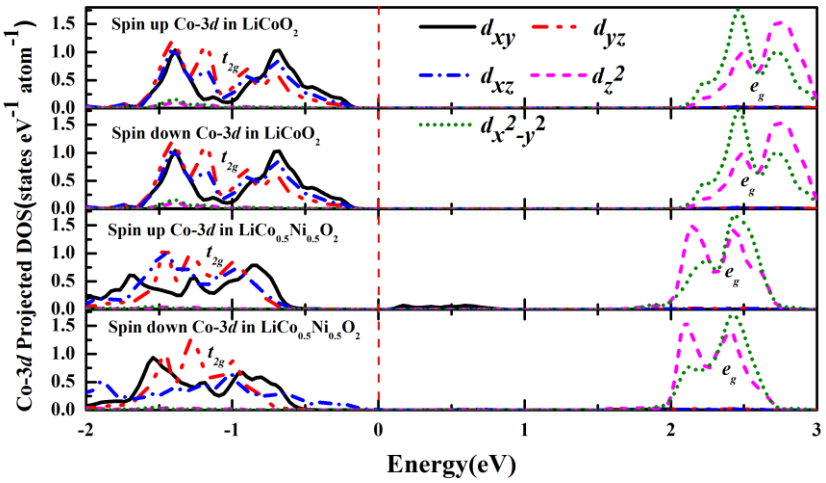

Figure 7. Co-3*d* PDOS in $LiCoO_2$ and $LiCo_{0.5}Ni_{0.5}O_2$. The triplet and the duplet of the *d*-orbital are denoted as t_{2g} and e_g, respectively. The Fermi levels are all set to be 0 eV.

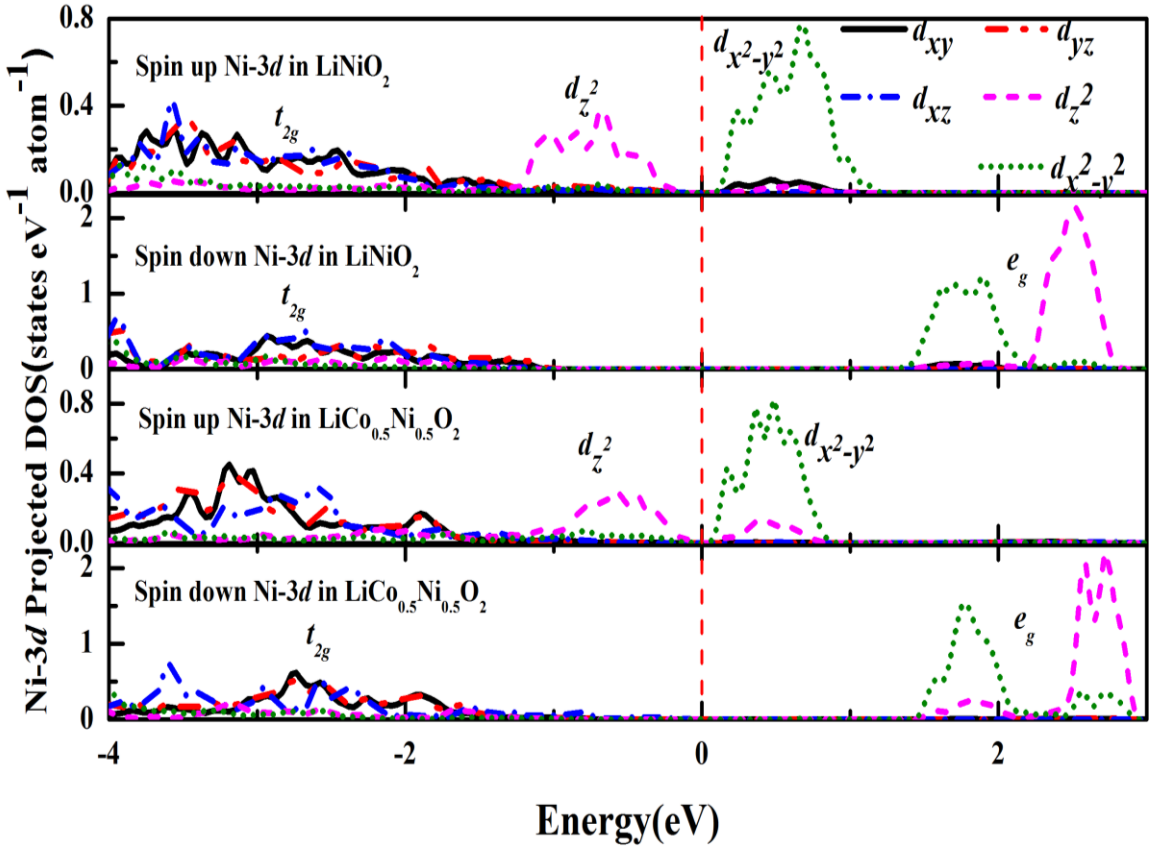

Figure 8. Ni-3*d* PDOS in $LiNiO_2$ and $LiCo_{0.5}Ni_{0.5}O_2$. The triplet and the duplet of the *d*-orbital are denoted as t_{2g} and e_g, respectively. The Fermi levels are all set to be 0 eV.

3.3 Formation energy

In order to evaluate the thermodynamical stability of the lithium mixed transition metal oxides compared to the simple Li*M*O_2 (*M* = Co, Mn, Ni) compound, we define the formation energy ΔE_{form} as following

$$\Delta E_{form}(LiM^{(1)}_{0.5}M^{(2)}_{0.5}O_2)=E(LiM^{(1)}_{0.5}M^{(2)}_{0.5}O_2)-1/2(E(LiM^{(1)}O_2)+E(LiM^{(2)}O_2)) \quad (1)$$

where $M^{(1)}$ and $M^{(2)}$ represent the different transition metal atoms, and $E(LiM^{(1)}_{0.5}M^{(2)}_{0.5}O_2)$, $E(LiM^{(1)}O_2)$ and $E(LiM^{(2)}O_2)$ are the total energies of $LiM^{(1)}_{0.5}M^{(2)}_{0.5}O_2$, $LiM^{(1)}O_2$ and $LiM^{(2)}O_2$, respectively.

Actually, according to the general alloy theory [38], the definition of formation energy represents a measure of the effective $M^{(1)}$ and $M^{(2)}$ interactions when they are mixed. If ΔE_{form} is negative, $M^{(1)}$ and $M^{(2)}$ have an effective attractive interaction and the system could be either mixed or ordered, which depends on the strength of the interaction and the preparation temperature. If ΔE_{form} is positive, however, local phase separation into $M^{(1)}$ and $M^{(2)}$ rich regions is energetically preferred.

The calculated formation energy of $LiMn_{0.5}Ni_{0.5}O_2$, $LiCo_{0.5}Ni_{0.5}O_2$ and $LiMn_{0.5}Co_{0.5}O_2$ are listed in Table 4. And the corresponding total energies for per formula unit are also given.

Table 4. The calculated total energies and formation energies of the formula units.

$LiMn_{0.5}Ni_{0.5}O_2$ (eV/f.u.)	$LiMnO_2$ / $LiNiO_2$ (eV/f.u.)	ΔE_{form}(meV)
-23.661	-26.411 / -20.156	-377
$LiCo_{0.5}Ni_{0.5}O_2$ (eV/f.u.)	$LiCoO_2$ / $LiNiO_2$ (eV/f.u.)	
-21.294	-22.419/ -20.156	-6
$LiMn_{0.5}Co_{0.5}O_2$ (eV/f.u.)	$LiMnO_2$ / $LiCoO_2$ (eV/f.u.)	
-24.477	-26.411/ -22.419	-62

As the lithium mixed transition metal oxides $LiM^{(1)}_{0.5}M^{(2)}_{0.5}O_2$ with the lowest energy adopt the rhombohedral structures, the rhombohedral structures of $LiM^{(1)}O_2$ and $LiM^{(2)}O_2$ are also taken into account as the references.

From Table 4, it can be found that the ΔE_{form} of $LiMn_{0.5}Ni_{0.5}O_2$, $LiCo_{0.5}Ni_{0.5}O_2$ and $LiMn_{0.5}Co_{0.5}O_2$ are all negative, indicating that the mixture of the transition metal are favorite for the three lithium mixed transition metal oxides. Among them, the formation energy of $LiMn_{0.5}Ni_{0.5}O_2$ (-377 meV per formula unit) is the lowest, which means that a strong ordering (attractive) tendency between Ni and Mn. Our calculated formation energy of $LiMn_{0.5}Ni_{0.5}O_2$ is somewhat lower than that of previous study (-216 meV per formula unit) [31], which is probably because the selected structures for $LiMnO_2$ and $LiNiO_2$ in their study are different from our structures. In contrast to the case of $LiMn_{0.5}Ni_{0.5}O_2$, the formation energy of $LiCo_{0.5}Ni_{0.5}O_2$ is much higher, which is about -6 meV per formula unit. The high formation energy suggests that phase separation is relatively easy to occur though Co and Ni could be mixed in the $LiCo_{0.5}Ni_{0.5}O_2$. Compared with $LiCo_{0.5}Ni_{0.5}O_2$ and $LiMn_{0.5}Ni_{0.5}O_2$, $LiMn_{0.5}Co_{0.5}O_2$ has a modest formation energy of -62 meV per formula unit. According to the calculated formation energies, therefore, $LiMn_{0.5}Ni_{0.5}O_2$ is most likely to be prepared among the three lithium mixed transition metal oxides.

4. CONCLUSIONS

In summary, we study the structures, electronic structures, charge transfer, electronic configuration, valence states and magnetic moment of $LiMn_{0.5}Ni_{0.5}O_2$, $LiMn_{0.5}Co_{0.5}O_2$ and $LiCo_{0.5}Ni_{0.5}O_2$ systems using the GGA+U methods within the DFT frame. Total energy calculations indicate that the rhombohedral structure is more stable than monoclinic one for all the three compounds $LiMn_{0.5}Ni_{0.5}O_2$, $LiMn_{0.5}Co_{0.5}O_2$ and $LiCo_{0.5}Ni_{0.5}O_2$. Bond length analysis shows that the Jahn-Teller effect disappears in Mn-containing compounds $LiMn_{0.5}Ni_{0.5}O_2$ and $LiMn_{0.5}Co_{0.5}O_2$, while the Jahn-Teller distortion still exist in $LiCo_{0.5}Ni_{0.5}O_2$, but mitigated to some extent. According to the electronic results, charge transfers from Mn ion to Ni (Co) ion, which results in forming Mn^{4+} and Ni^{2+} (Co^{2+}), is the main reason of the suppression in $LiMn_{0.5}Ni_{0.5}O_2$ and $LiMn_{0.5}Co_{0.5}O_2$. In $LiCo_{0.5}Ni_{0.5}O_2$, however, no charge transfer between Co and Ni could be observed. The TDOS results indicates that $LiMn_{0.5}Ni_{0.5}O_2$, $LiMn_{0.5}Co_{0.5}O_2$ and $LiCo_{0.5}Ni_{0.5}O_2$ are all semiconducting with smaller energy band

gaps compared with the single phase LiMO_2 (M = Co, Ni, Mn). In addition, formation energy calculations show that $LiMn_{0.5}Ni_{0.5}O_2$, $LiMn_{0.5}Co_{0.5}O_2$ and $LiCo_{0.5}Ni_{0.5}O_2$ compounds are thermodynamics stable when compared to the basic layered LiMO_2 (M = Co, Mn, Ni). Therefore, the mixture of cations in the lithium transition metal oxides could be formed, and the order for the mixture from easy to difficult is $LiMn_{0.5}Ni_{0.5}O_2$ > $LiMn_{0.5}Co_{0.5}O_2$ > $LiCo_{0.5}Ni_{0.5}O_2$.

ACKNOWLEDGEMENTS
This work is supported by the Natural Science Foundation of China under Grand Nos. 11264014 and 11564016, and Natural Science foundation of Jiangxi Province under Grand No. 20133ACB21010, 20142BAB212002 and 20152ACB2101. B. Xu is also supported by the oversea returned project from the Ministry of Education.

References

1. R. Koksbang, J. Barker, H. Shi and M. Y. Saidi, *Solid State Ionics*, 84 (1996) 1.
2. T. Ohzuku, A. Ueda and M. Nagayama, *J. Electrochem. Soc*., 140 (1993) 1862.
3. A. Hirano, R. Kanno, Y. Kawamoto, K. Oikawa, T. Kamiyama and F. Izumi, *Solid State Ionics*, 791 (1996) 86.
4. M. Saiful Islam and R. Andrew Davies, *Chem. Mater*., 15 (2003) 4280.
5. P. G. Bruce, *Chem. Commun*., 19 (1997) 1817.
6. M. M. Thackeray, *Prog. Solid State Chem*., 25 (1997) 1.
7. M. S. Whittingham and P. Y. Zavalij, *Solid State Ionics*, 131 (2000) 109.
8. B. Ammundsen and J. Paulsen, *Adv. Mater*., 13 (2001) 943.
9. G. Amatucci and J. M. Tarascon, *J. Electrochem. Soc*., 149 (2002) K31.
10. T. Ohzuku, A. Ueda, M. Nagayama, Y. Iwakoshi and H. Komori, *Electrochim. Acta*, 38 (1993) 1159.
11. M. Broussely, J. P. Planchat, G. Rigobert, D. Virey and G. Sarre, *J. Power Sources*, 68 (1997) 8.
12. J. P. Cho, H. S. Jung, Y. C. Park, G. B. Kim and H. S. Lim, *J. Electrochem. Soc*., 147 (2000) 15.
13. Hernan, A. Caballero, J. Morales, E. R. Castellon and J. Santos, *J. Power Sources*, 128 (2004) 286.
14. R. Stoyanova, E. Zhecheva and L. Zarkova, *Solid State Ionics*, 73 (1994) 233.
15. Y. Koyama, Y. Makimura, I. Tanaka, H. Adachi and T. Ohzuku, *J. Electrochem. Soc*., 151 (2004) A1499.
16. N. N. Shukal, S. Shukal, R. Prasad and R. Benedek, *Modelling Simul. Mater. Sci. Eng*., 16 (2008) 055008.
17. J. M. Wang, J. P. Hu, C. Y. Ouyang, S. Q. Shi and M. S. Lei, *Solid State Commun.*, 151 (2011) 234.
18. S. Hao, N. Q. Zhao, C. S. Shi, C. N. He, J. J. Li and E. Z. Liu, *Ceram. Int.*, 41 (2015) 2294
19. E. Rossen, C. D. W. Jones and J. R. Dahn, *Solid State Ionics*, 57 (1992) 311.
20. T. Ohzuku and Y. Makimura, *Chem. Lett*., 8 (2001) 744.
21. P. Senthil Kumar, A. Sakunthala, M. Prabu, M. V. Reddy, R. Joshi, *Solid State Ionics*, 267 (2014) 1.
22. G. Kresse and J. Furthmuller, *Phys. Rev. B*, 54 (1996) 11169.
23. G. Krosse and J. Joubert, *Phys. Rev. B*, 59 (1999) 1758.
24. J. P. Perdew, K. Burke and M. Ernzerhof, *Phys. Rev. Lett*., 77 (1991) 3865.
25. V. I. Anisimov, J. Zaanen and O. K. Andersen, *Phys. Rev. B*, 44 (1991) 943.
26. I. V. Solovyev, P. H. Dederichs and V. I. Anisimov, *Phys. Rev. B*, 50 (1994) 16861.
27. F. Zhou, K. Kang, T. Maxisch, G. Ceder and D. Morgan, *Solid State Commun.*, 132 (2004) 181.

28. H. J. Monkhorst and J. D. Pack, *Phys. Rev. B*, 13 (1976) 5188.
29. Y. Kim, *J. Mater. Sci*., 47 (2012) 7558.
30. A. Dianat, N. Seriani, M. Bobeth and G. Cuniberti, *J. Mater. Chem. A*, 1 (2013) 9273.
31. J. Reed, G. Ceder, *Electrochem. Solid State Lett*., 5 (2002) A145.
32. C. S. Johnson, J. S. Kim, A. J. Kropf, A. J. Kahaian, J. T. Vaughey, L. M. L. Fransson, K. Edström and M. M. Thackeray, *Chem. Mater*., 15 (2003) 2313.
33. T. Ohzuku and Y. Makimura, *Res. Chem. Intermed*., 32 (2006) 507.
34. R. Prasad, R. Benedek, M. M. Thackeray, *Phys. Rev. B*, 71 (2005) 134111.
35. Z. L. Chen, H. M. Zou, X. P. Zhu, J. Zou, J. F. Cao, *J. Solid State Chem*., 184 (2011) 1784.
36. R. Prasad, R. Benedek, A. J. Kropf, C. S. Johnson, A. D. Robertson, P. G. Bruce and M. M. Thackeray, *Phys. Rev. B*, 68 (2003) 012101.
37. F. Xiong, H. J. Yan, Y. Chen, B. Xu, J. X. Le, C. Y. Ouyang, *Int. J. Electrochem. Sci.*, 7 (2012) 9390
38. D. de Fontaine, *Solid State Phys.*, Academic Press, New York, 47 (1994) 33.